Final Report to

Gyroscope Guidance Sensor for Ultra-Deepwater Applications 09121-3500-10.Final

July 24, 2013

Chopin Hua, PI
Laserlith Corporation
4200 James Ray Drive, Ste 501
Grand Forks, ND 58203
laserlithco@aol.com

LEGAL NOTICE

This report was prepared by Laserlith Corporation as an account of work sponsored by the Research Partnership to Secure Energy for America, RPSEA. Neither RPSEA members of RPSEA, the National Energy Technology Laboratory, the U.S. Department of Energy, nor any person acting on behalf of any of the entities:

a. MAKES ANY WARRANTY OR REPRESENTATION, EXPRESS OR IMPLIED WITH RESPECT TO ACCURACY, COMPLETENESS, OR USEFULNESS OF THE INFORMATION CONTAINED IN THIS DOCUMENT, OR THAT THE USE OF ANY INFORMATION, APPARATUS, METHOD, OR PROCESS DISCLOSED IN THIS DOCUMENT MAY NOT INFRINGE PRIVATELY OWNED RIGHTS, OR

b. ASSUMES ANY LIABILITY WITH RESPECT TO THE USE OF, OR FOR ANY AND ALL DAMAGES RESULTING FROM THE USE OF, ANY INFORMATION, APPARATUS, METHOD, OR PROCESS DISCLOSED IN THIS DOCUMENT.

THIS IS A FINAL REPORT. THE DATA, CALCULATIONS, INFORMATION, CONCLUSIONS, AND/OR RECOMMENDATIONS REPORTED HEREIN ARE THE PROPERTY OF THE U.S. DEPARTMENT OF ENERGY.

REFERENCE TO TRADE NAMES OR SPECIFIC COMMERCIAL PRODUCTS, COMMODITIES, OR SERVICES IN THIS REPORT DOES NOT REPRESENT OR CONSTIITUTE AND ENDORSEMENT, RECOMMENDATION, OR FAVORING BY RPSEA OR ITS CONTRACTORS OF THE SPECIFIC COMMERCIAL PRODUCT, COMMODITY, OR SERVICE.

SIGNATURE AND DATE STAMP

_____

CHOPIN HUA, PI

_____

DATE

1. ABSTRACT

The team designed an inertial guidance system for ultra-deepwater drilling. The system was based on MEMS gyroscope technology; with a demonstrated gyroscope mechanical sensor design integrated with robust readout circuits that can operate in the down-hole environment, ie. high temperature and high vibration/shock. MEMS gyroscopes enable this inertial guidance system to be positioned next to the drill bit, which is a significant improvement over existing magnetometer guidance systems that must be installed 50 to 80 feet behind the drill bit. The shortened reaction reduces drilling time and drilling cost. The system could potentially enable a greater volume of the reservoir to be accessed from a single surface location, decreasing costs and environmental impact.

2. TABLE OF CONTENTS

SIGNATURE AND DATE STAMP 4

1. ABSTRACT 5

2. TABLE OF CONTENTS 6

3. FIGURES AND TABLES 7

4. EXECUTIVE SUMMARY 8

5. REPORT DETAILS 10

5.1 Experimental Methods: 10
5.1.1 Control Circuit Design 10
5.1.2 MEMS Optimization 13
5.1.3 Gyroscope Module Assembly 14
5.1.4 Testing 16

5.2 Results and Discussions: 16
5.2.1 Drive Circuit Measurements 16
5.2.2 MEMS Fabrication 19
5.2.3 Integration and Testing 22
5.2.4 Noise Filtering / Cancellation 23
5.2.5 Impact to Producers 24
5.2.6 Technology Transfer Efforts 25

5.3 Conclusions and Recommendations 26
Gyroscope System Improvements 27

6. BIBLIOGRAPHY 28

7. LIST OF ACRONYMS AND ABBREVIATIONS 29

8. APPENDICES 29

9. REFERENCES 30

3. FIGURES and TABLES

FIGURE 1. SCHEMATIC OF (A) DRIVE AND (B) SENSE CIRCUIT FOR MEMS GYROSCOPE. 11
FIGURE 2. THE MEASUREMENT OF THE INPUT LOSS. 12
FIGURE 3. SIMULATION OF THE INPUT LOSS 13
FIGURE 4. MEMS SENSOR FABRICATION PROCESS FLOW. 13
FIGURE 5. IN-HOUSE SEMICONDUCTOR FABRICATION EQUIPMENT FOR THE MEMS SENSOR PROCESS. 14
FIGURE 6. DESIGN AND COMPONENTS OF THE GYROSCOPE MODULE. 15
FIGURE 7. SIDE VIEW OF MICROBUMP INTERCONNECTED SENSOR: THE PROCESS ENABLES A 'DIVIDE AND CONQUER' 15
FIGURE 8. TEAM MEMBER IDEAL AEROSMITH HAS SUBSTANTIAL EXPERIENCE IN THE TESTING OF GYROSCOPES FOR THE OIL DRILLING APPLICATION. IDEAL AEROSMITH ALSO DEVELOPS, PRODUCES AND SELLS TEST EQUIPMENT INCLUDING RATE TABLES. 16
FIGURE 9. THE MEASUREMENT RESULTS OF THE DRIVE CIRCUIT WITH I_{P1} = 0.1 MA 17
FIGURE 10. THE MEASUREMENT RESULTS OF THE DRIVE CIRCUIT WITH I_{P1} = 1 μA 18
FIGURE 11. THE MEASUREMENT RESULTS OF THE DRIVE CIRCUIT WITH I_{IN} = 0.4 MA 18
FIGURE 12. THE MEASUREMENT RESULTS OF THE DRIVE CIRCUIT WITH I_{IN} = 2 μA 18
FIGURE 13. THE MEASUREMENT RESULTS OF THE DRIVE CIRCUIT WITH I_{IN} = 0.1 μA 19
FIGURE 14. SILICON DRIE ETCH WITH THE THICKER DEVICE SILICON LAYER. 19
FIGURE 15. SEM IMAGES OF BLACK SILICON AT THE BOTTOM OF A TRENCH FORMING GRASS-LIKE STRUCTURES. 20
FIGURE 16. LEFT: SMALLER FEATURES UNDER-ETCHED THROUGH THE SILICON DEVICE LAYER. ADJUSTMENTS TO THE PROCESS PARAMETERS WERE NEEDED TO BRING THE PROCESS BACK TO SPECIFICATION. RIGHT: ETCH CROSS SECTION PROFILE. THE RED DOTTED LINE REPRESENTS THE DESIRED ETCH PROFILE. 21
FIGURE 17. MICROGRAPH SHOWING THE SMALLER FEATURES WERE NOT BEING ETCHED ALL THE WAY THROUGH THE SILICON DEVICE LAYER. 21
FIGURE 18. AFTER ADJUSTING THE RF AND CYCLE STEPS, SILICON LAYERS WERE SUCCESSFULLY ETCHED. 22
FIGURE 19. DESIGNED PRINTED CIRCUIT BOARD, WHICH CONTAINS THE GYROSCOPE MECHANICAL SENSING ELEMENT AND FRONT-END LOW-NOISE AMPLIFICATION STAGES. THE MODULE IS 0.75" DIAMETER AND REQUIRES JUST 5 VOLTS POWER WITH A POWER CONSUMPTION OF 25MW. 22
FIGURE 20. ROTATION RATE MEASUREMENT 23
FIGURE 21. DESIGN OF THE CHIP CAROUSELING TO CANCEL THE 1/F NOISE. 23

TABLE 1. INPUT AND OUTPUT SIGNALS OF THE DRIVE CIRCUIT BETWEEN SIMULATION AND MEASUREMENT 17
TABLE 2. GYRO REPLACEMENT COST SAVINGS TABLES 25

4. EXECUTIVE SUMMARY

The team designed an inertial guidance system for ultra-deepwater drilling. The system was based on MEMS gyroscope technology, with a demonstrated gyroscope mechanical sensor design integrated with robust readout circuits that can operate in the down-hole environment, ie. high temperature and high vibration/shock. MEMS gyroscopes enable this inertial guidance system to be positioned next to the drill bit, which is a significant improvement over existing magnetometer guidance systems that must be installed 50 to 80 feet behind the drill bit. The shortened reaction reduces drilling time and drilling cost. The system could potentially enable a greater volume of the reservoir to be accessed from a single surface location, decreasing costs and environmental impact.

The three main components to the work included high temperature circuit design, optimization of the MEMS sensing element, assembly and test.

The control electronics were upgraded with new circuit components that are smaller and can handle the higher temperatures that would be seen in down-hole drilling environment.

Development work began with optimization of the mechanical sensing element. Work focused on increasing the thickness of the sensing element to make the MEMS sensing structure more robust. The area of the electrostatic combs was also increased, reducing stiction and improving sensitivity. Increasing the thickness of the device makes the silicon etching process more challenging and therefore process development and qualification runs were completed to insure the gyroscope could be manufactured to the design specifications. There were some glitches in the processing of the MEMS sensing element, including equipment malfunctions and process modifications. Work is ongoing to continuously improve the design as well as new fabrication iterations of the sensing element.

The MEMS and electronics were successfully integrated into a circuit board module with successful test results. Work is ongoing to improve the module assembly. The team is also focused on improving device yield and performance. Additional improvements were made in the manufacturing process to reduce cost and increase speed.

The successful development of this technology can substantially reduce response time of drilling measurements by providing the ability to install the inertial sensor next to the drill bit. Improved accuracy and reduced drilling time accelerates the rate of commercial production, as well as exploration in emerging plays. A MEMS gyro can significantly reduce drilling time for casing window cutting applications, intermediate radius re-entry applications and steering applications.

Finally, the team intends to develop, produce, market, sell, and support MEMS-based inertial guidance systems for directional drilling. The team includes the necessary development, manufacturing and support capabilities in-house, and is coordinating system development with oil drilling equipment companies.

Tasks	Results
MEMS Gyroscope Design	Optimized and fabricated
Control Electronics	Improved design with high temperature components
Gyroscope Module	Module designed and built. The MEMS sensor is still being fabricated.

5. REPORT DETAILS

The Laserlith team designed an inertial guidance system with a high angle north-seeking gyroscope that is compatible with the down-hole operation temperatures of up to 130° with a gyroscope compass accuracy of better than 0.1°. The MEMS sensor is still being fabricated.

5.1 Experimental Methods:

The project was broken down to three specific areas:

1. CONTROL CIRCUIT
2. MEMS OPTIMIZATION
3. GYROSCOPE TESTBED: MEMS-Circuit integration

5.1.1 Control Circuit Design

The primary components of the control electronics consists of a gyro driver circuit, and sense circuit. The development of these components is described in the following sections. A schematic of the drive and sense circuits are shown in Figure 1.

The gyro driver circuit supplies the drive oscillation signal to the MEMS gyroscope and maintaining it at a constant level. Changes in the environmental conditions can cause the gyro oscillation amplitude to shift and the circuit minimizes drift to get accurate measurements. The driver circuit features closed loop feedback control that maintains the gyroscope drive signal. The signal is fed to the gyroscope and is read back on the gyro's drive sense combs to measure the oscillation amplitude.

The gyro sense circuit measures the Coriolis response of the gyroscope. It amplifies the small output signal from the gyroscope to higher levels which can than be processed by a microcontroller circuit. The sense circuit also includes noise filtering.

Both the drive and sense circuit boards include sockets for the discrete electronic components to give the flexibility to swap parts and tune the circuit's signal manipulation to achieve the best performance.

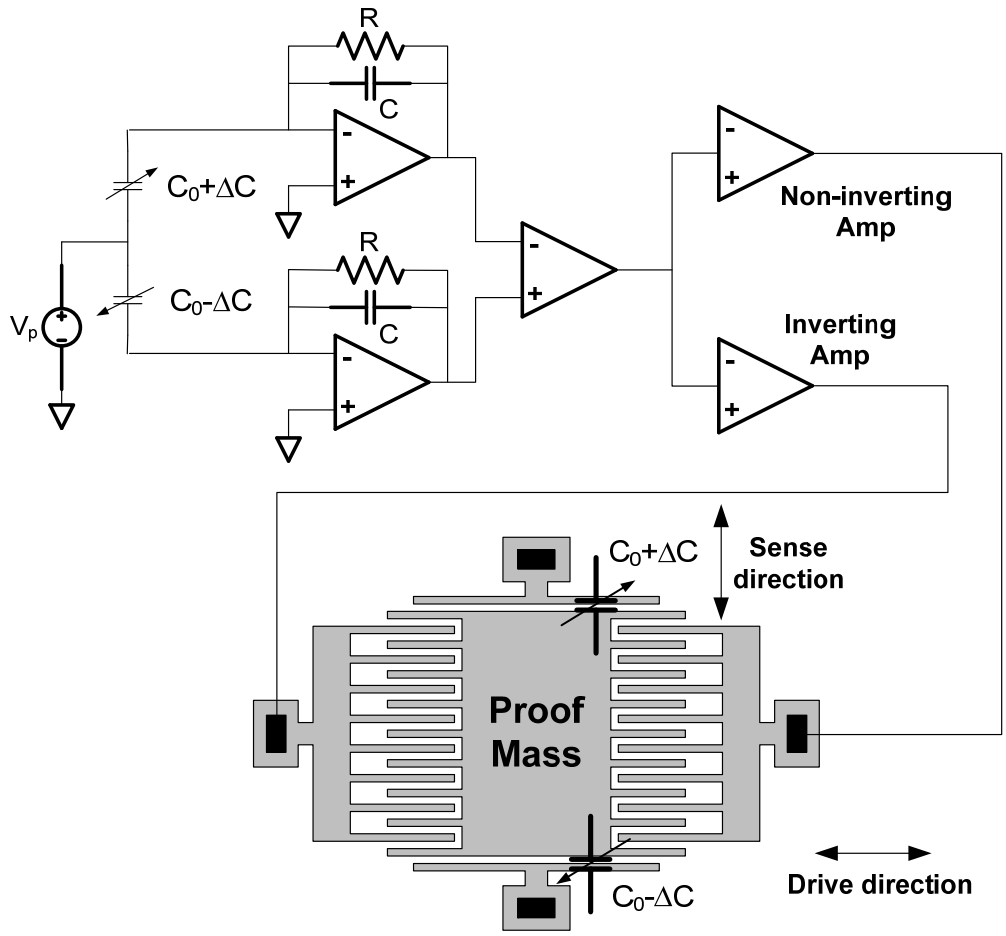

(a)

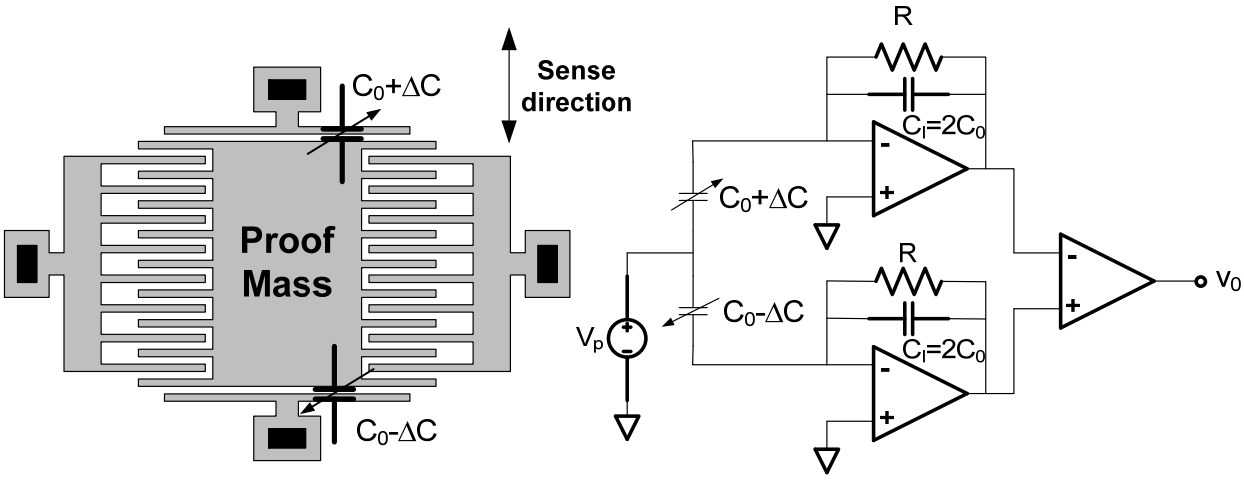

(b)

Figure 1. Schematic of (a) drive and (b) sense circuit for MEMS gyroscope.

Additional components included a high-pass filter after the second stage to filter the low-frequency noise. An inverter amplifier and a non-inverter amplifier are placed as the third stage to amplify the signals and provide the complementary output signals. Due to the lower output gain of previous drive circuit designs with the feedback resistance of 100 KΩ, the feedback resistance changed back to 1 MΩ to enhance the first-stage gain from 70 back to 100. To decrease the low-frequency noise amplified in the first stage, the high-pass filter with 2.2 KΩ and 3.3 nF placed at the second-stage. Therefore, the theoretical output gain of the sense circuit and the drive circuit are shown below:

$$\text{Sense Circuit Gain} = 100 \times 200 = 20000 = 86\ \text{dB}$$

$$\text{Drive Circuit Gain} = 100 \times 200 \times 100 = 126\ \text{dB}$$

The V_{DD} and V_{SS} of the operational amplifiers in the sense circuit are 5V and 0V, respectively. The biased ground of the drive circuit is shifted from 0 V to 2.5 V to prevent the signals from being clipped by the supply DC voltages. 2.2 KΩ resistors and 3.3 nF capacitors were replaced by the previous 1 KΩ resistors and worked as a high-pass filter to filter the low frequency noises. Also, the DC bias from the AC signal source is not necessary in this configuration. In the input stages, small capacitors are added in front of the input stage, 1 pF in this case, for the measurement to filter the low frequency noise which might come from the AC current source. In addition, the input series capacitance is small enough to decrease the input signal level of the AC current so that the smaller input current become possible. The measured input loss by the 1 pF input capacitor is about 19.3 mV / 3.25 = 0.006, which is larger than the simulation value of 0.001. The difference of the results might be come from the measurement error, but the input capacitor still can used for reduce the input level. Both the results are shown as Figure 2 and Figure 3. Note that the signal distributed after passing the input 1 pF capacitor.

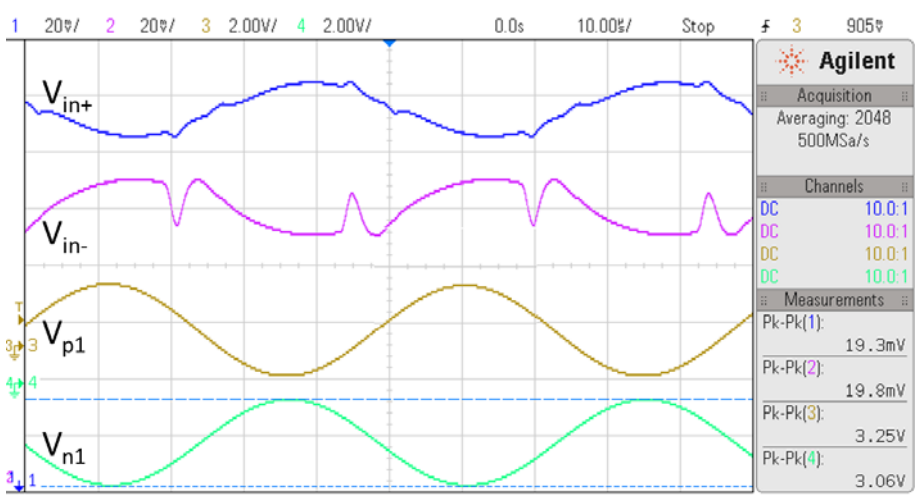

Figure 2. The measurement of the input loss.

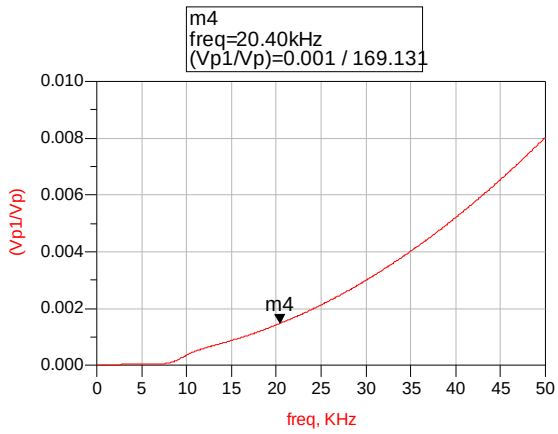

Figure 3. Simulation of the input loss

5.1.2 MEMS Optimization

Figure 4 shows the process flow for the fabrication of the MEMS. Steps include lithography, metallization and dry reactive ion etch. All steps are processed on-site with in-house equipment (Figure 5).

Figure 4. MEMS Sensor Fabrication Process flow.

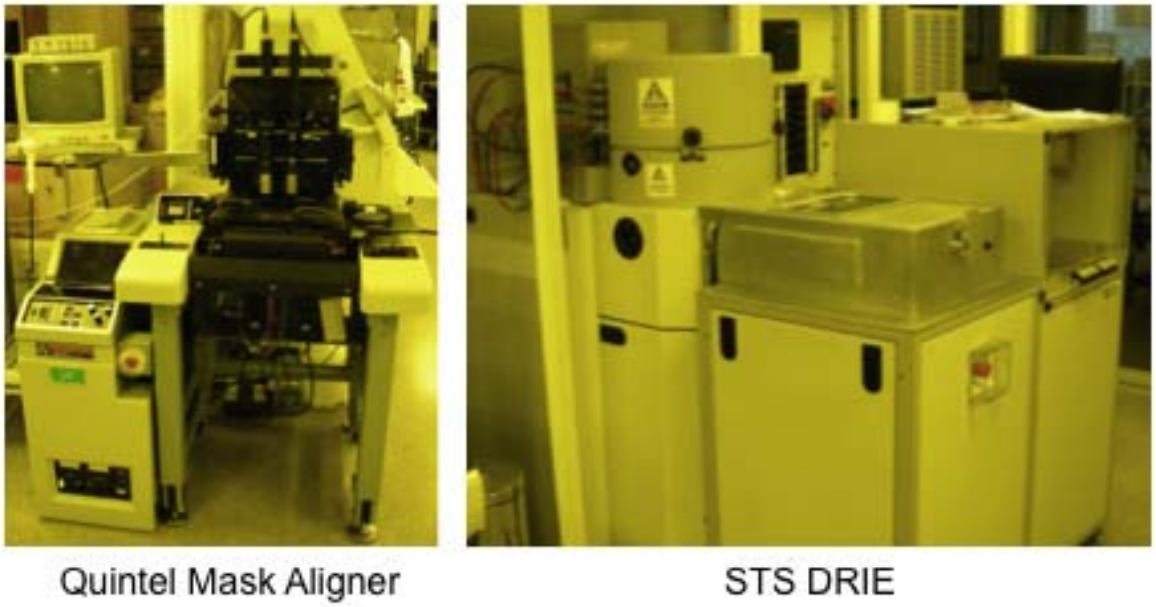

Figure 5. In-house semiconductor fabrication equipment for the MEMS sensor process.

Material Optimization

Switching to SOI wafers with a 50-100um thick device layer was evaluated. A thicker gyro sensing element will be stiffer in the out of plane non-sensing axis and will lead to a lower risk of failure due to stiction. The area of the electrostatic combs will also increase and therefore increase gyro sensitivity. Based on the formula:

$$\text{Capacitance} = \varepsilon A / d$$

It was determined that working with a 5x thicker SOI which gives a 5x increase in sensitivity.

Optimizing the thickness of the buried oxide layer (BOX) was another option that was evaluated. By increasing the thickness, a larger gap will be created between the mechanical sensing element and handle substrate. This reduces the chance of stiction and can reduce sensor noise levels. Possible problems with using a thicker BOX layer include a greater chance of uneven oxide etch and reduced strength at the silicon device layer anchor points.

SOI wafers with a thicker BOX layer were processed using the standard silicon DRIE etch to create test structures for qualification. The structure was examined using an IR microscope to view the oxide etch profile. A uniform etch boundary was observed, confirming that oxide was successfully etched. The anchor points were tested for strength by applying a shear force on the silicon device layer. The anchor withstood the applied force without any observable failures.

5.1.3 Gyroscope Module Assembly

Once the Circuit and MEMS have been designed and fabricated, the components are integrated together as a hybrid assembly using the team's low-loss microbump process. Figure 7 illustrates the side view of an interconnected sensor. The key is the microbump interconnect that electrically interconnects the mechanical sensing

structure to the high temperature electronics with minimal parasitic losses (10 to 50 femtoFarads).

This unique proprietary approach enables the separate optimization of the sensor structure and the circuits for the oil drilling application. It is often desirable to improve the sensitivity of the gyroscope by increasing its sense mass (by increasing the thickness of the sense mass layer). With the ability to separately optimize the mechanical structure from the circuits, it is relatively straightforward to utilize a thicker sense mass layer without concern for damaging transistors on the same wafer. This 'divide and conquer' approach addresses several critical shortcomings of the integrated MEMS-IC process discussed above. This modular approach enables the 200C SOI CMOS circuit to be swapped out for the lower noise circuit.

The integrated chips are then wired into a high-temperature metal housing, complete with a separate rotation module to carousel the chips for 1/f noise cancellation. The Figure 6 shows the module design.

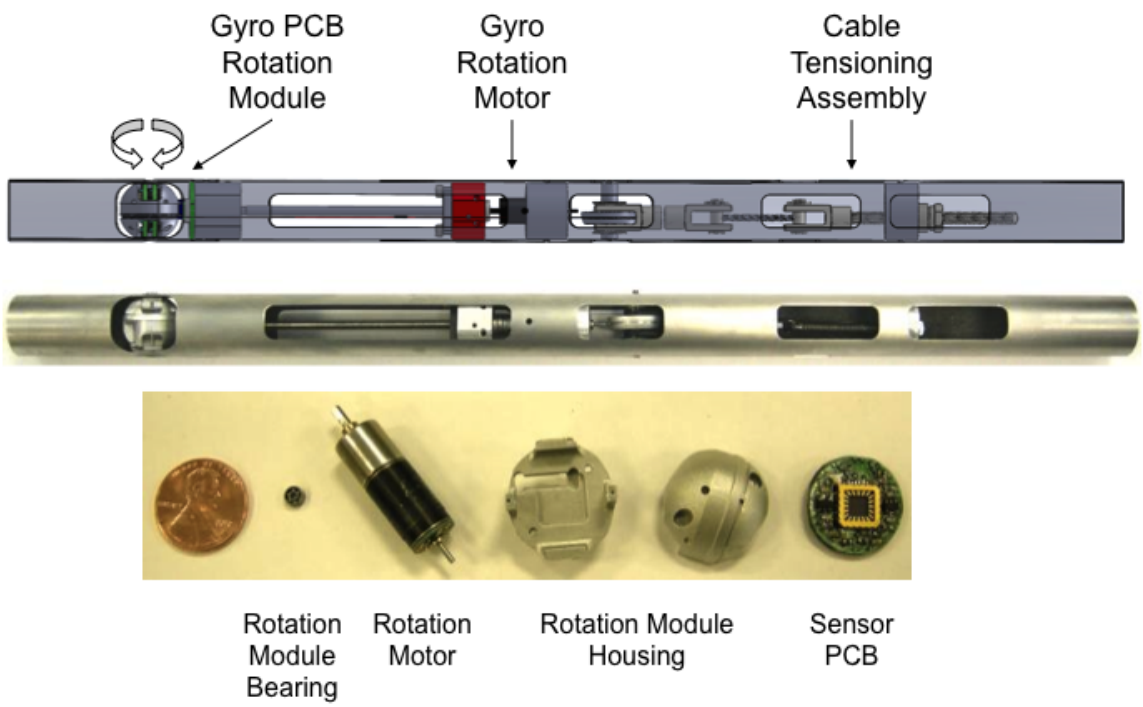

Figure 6. Design and components of the Gyroscope module.

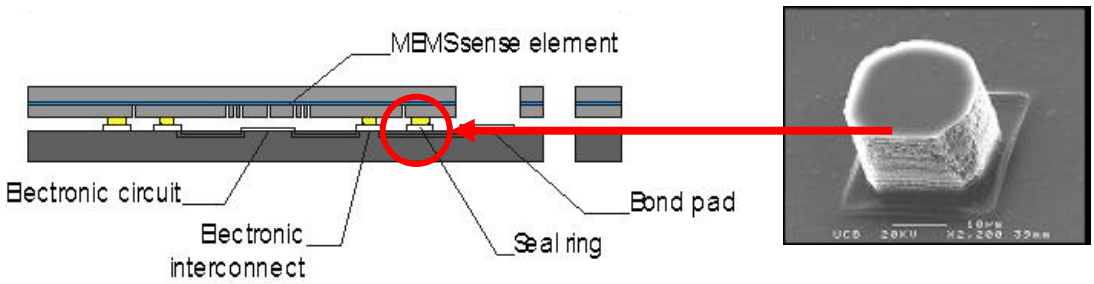

Figure 7. Side view of microbump interconnected sensor: The process enables a 'divide and conquer'

5.1.4 Testing

Both the sensor and the filter electronics require significant amounts of specialized test equipment in addition to the standard electronics resources found in a research lab. The initial testing is typically done on a standard single axis rate and positioning table like the Ideal Aerosmith Model 1291. The rate table provides a stable rate input to simulate speeds from earth rate to several thousand degrees/second. The system can also be equipped with a vacuum chamber for testing devices that have not yet been packaged.

The next level of testing is done on multi-axis rate and positioning tables with thermal systems such as the 2002P. These tables are used to ensure that the complete navigation package is operating properly. In addition to simulating rates in different axes, the system can simulate both hot and cold environments while subjecting the package to rate stimuli. Figure 8 shows a number of rate tables developed by team member Ideal Aerosmith for gyroscope testing and setup.

Figure 8. Team member Ideal Aerosmith has substantial experience in the testing of gyroscopes for the oil drilling application. Ideal Aerosmith also develops, produces and sells test equipment including rate tables.

5.2 Results and Discussions:

5.2.1 Drive Circuit Measurements

Table 1 shows the simulated and actual results of the input signals and the output results. The output signals of the sense circuit are equal to the output signals of the second-stage of the drive circuit. Note that the input AC current are different between the simulations and the measurements because there is only part of the current flowing into the drive circuit. However, the actual input and output signals of each circuit stages were almost perfectly matched as the simulation in the condition of the same input voltage. The measurement results of Table 1 are shown as Figure 9 to Figure 13. The simulated and measured gain of the circuits can be estimated from Table 1 as below:

Simulated Sense Circuit: 878 / 42 m = 86.40 dB

Measured Sense Circuit: (3.37/1μ)/(3.2/0.1m) x 2 x (1.792/19.3m) = 85.82 dB

Simulated Drive Circuit: 85640 / 42 m = 126.19 dB

Measured Drive Circuit: 19556 x (2.12/23.5m) = 124.93 dB

The gain estimated from the measurement results is lower than that in simulation due to the small scale measurement and estimation error. Nevertheless, the measured circuit gains are close to the simulation results.

Table 1. Input and output signals of the drive circuit between simulation and measurement

I_{in} (Simu.) I_{in} (Meas.)	I_{p1} (Simu.) I_{p1} (Meas.)	V_{p1} or V_{n1} (After 1 pF)	$V_{1st\text{-}stage}$	$V_{2nd\text{-}stage}$	V_{out}
	0.15mA peak 0.1 mA peak	3.44 Vpp 3.2 Vpp	300 Vpp Over 5 Vpp	73180 Vpp Over 5 Vpp	7136000 Vpp Over 5 Vpp
	1.5 mA peak 1 mA peak	34 mVpp 43.4 mVpp	3.00 Vpp 3.37 Vpp	732 Vpp Over 5 Vpp	71360 Vpp Over 5 Vpp
1.8 mA peak 0.4 mA peak		42 mVpp 44.8 mVpp	3.594 Vpp 3.57 Vpp	878 Vpp Over 5 Vpp	85640 Vpp Over 5 Vpp
3.5 nA peak 2 mA peak		80 mVpp X	6 mVpp (Diff) 19.3 mVpp	1.708 Vpp 1.792 Vpp	166 Vpp Over 5 Vpp
40 pA peak 0.1 mA peak		0.9 mVpp X	80 mVpp X	20 mVpp 23.5 mVpp	1.90 Vpp 2.12 Vpp

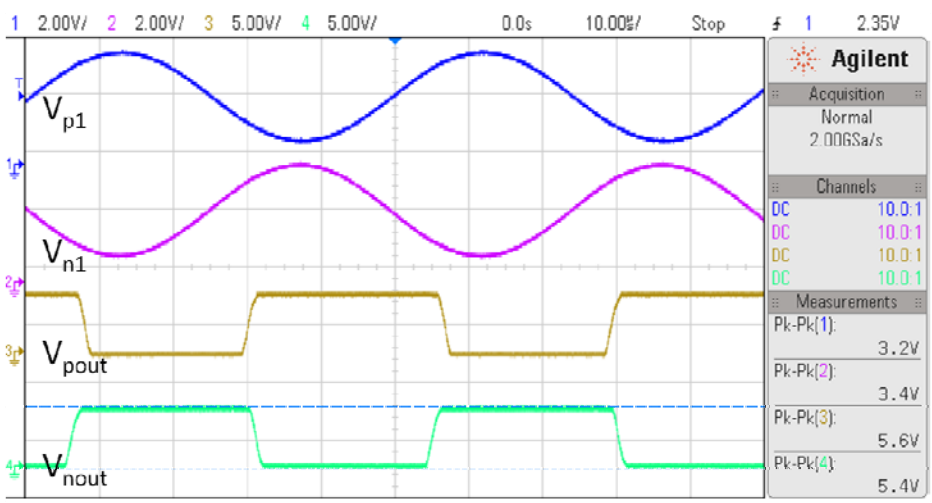

Figure 9. The measurement results of the drive circuit with I_{p1} = 0.1 mA

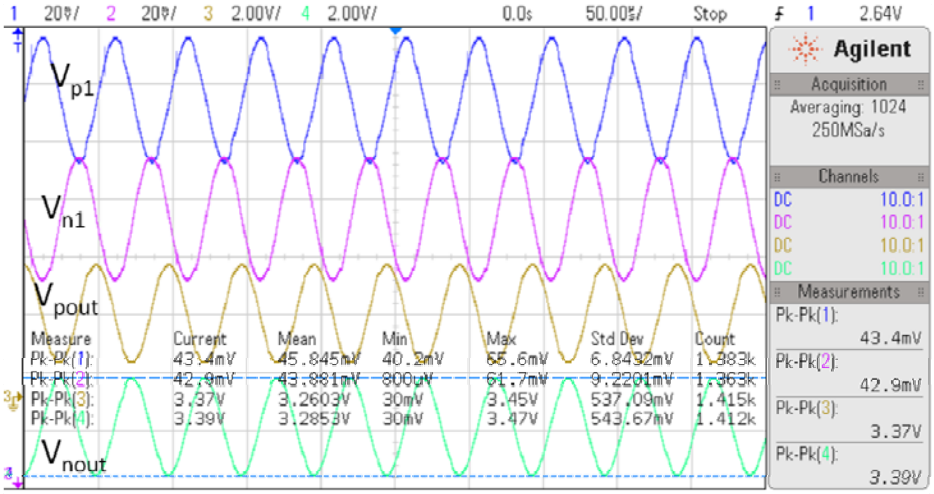

Figure 10. The measurement results of the drive circuit with I_{p1} = 1 μA

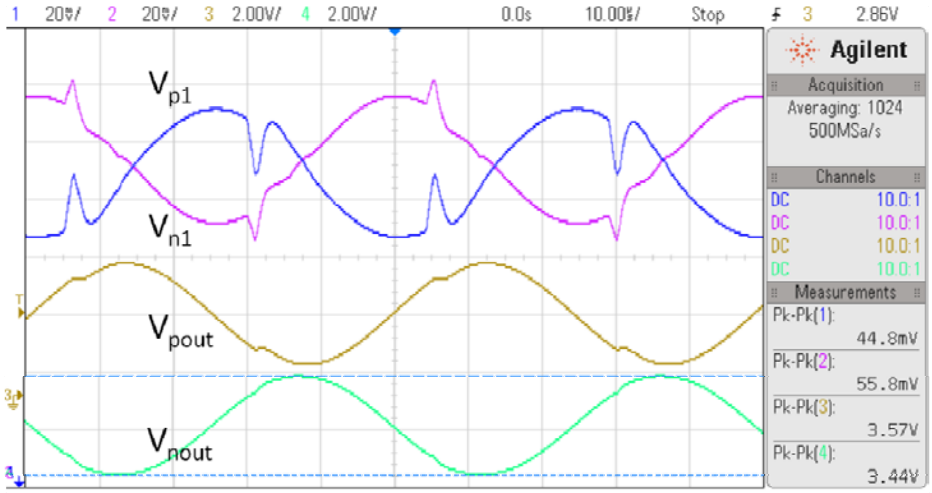

Figure 11. The measurement results of the drive circuit with I_{in} = 0.4 mA

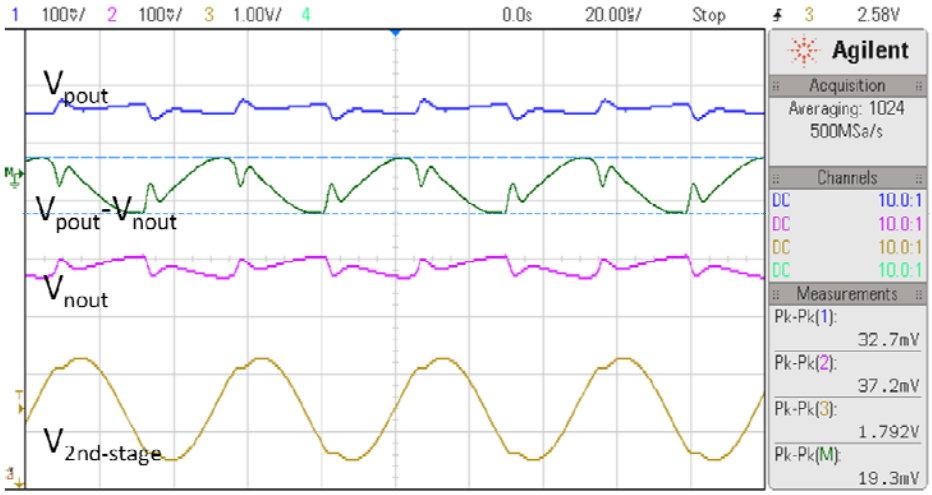

Figure 12. The measurement results of the drive circuit with I_{in} = 2 μA

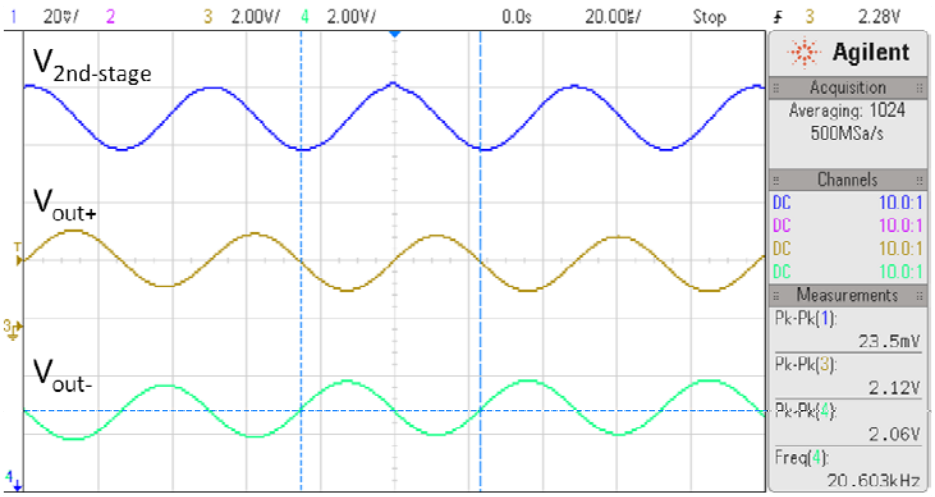

Figure 13. The measurement results of the drive circuit with I_{in} = 0.1 μA

5.2.2 MEMS Fabrication

5.2.2.1 Black Silicon

Some qualifications runs were performed to tune the fabrication tools and verify that thicker wafers can be used. The gyroscope sensing element is formed by a Deep Reactive-Ion Etching (DRIE) tool that cuts out deep trenches with near vertical sidewalls into silicon. By using a thicker silicon layer, the DRIE process must be tested to insure that the trenches can be successfully etched all the way through the silicon. Test structures were etched into the thicker SOI wafer and inspected to determine the etch performance (Figure 14).

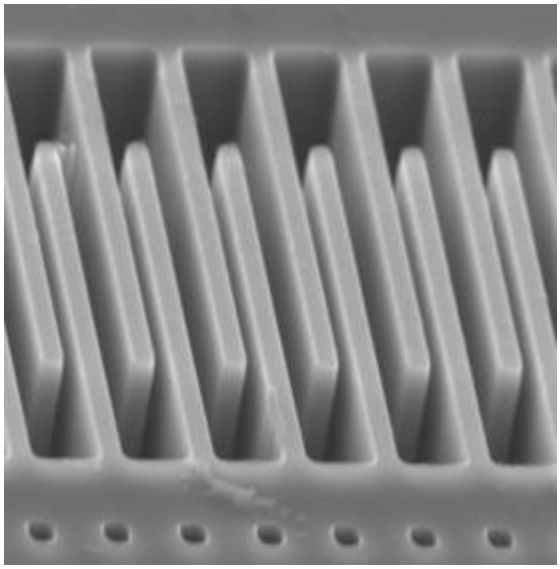

Figure 14. Silicon DRIE etch with the thicker device silicon layer.

When dialing in the DRIE process for the MEMS device, the first step is to optimize the etch selectivity of silicon versus photoresist. In order to etch 50-100 μm with a photoresist mask of roughly 1-2 micron thickness, an overall etch selectivity of at least 50:1 is needed. The etch selectivity throughout the process depends on depth as well as feature size. Deeper etches or smaller feature sizes will require greater selectivity. This determined the maximum device layer thickness that can be used for the gyroscopes.

An initial etch selectivity 100:1 was reached, but when etching the test wafers, some black silicon formed in the bottom of the trenches. Black silicon (Figure 15) is a condition in which many small spires of silicon are formed when small specs of oxide or photoresist gets deposited onto the silicon thereby blocking the ions and keeping those areas from being etched. The deeper the etch, the higher the probability of the formation of black silicon. Significant development work was spent on solving this problem, which included changing process parameters for plasma generator frequency and power (coil), vacuum pressure level, platen temperature, etch rates, and gas flow levels. After tweaking the process by increasing the coil and platen power, the black silicon no longer appeared, but the initial selectivity decreased to 90:1.

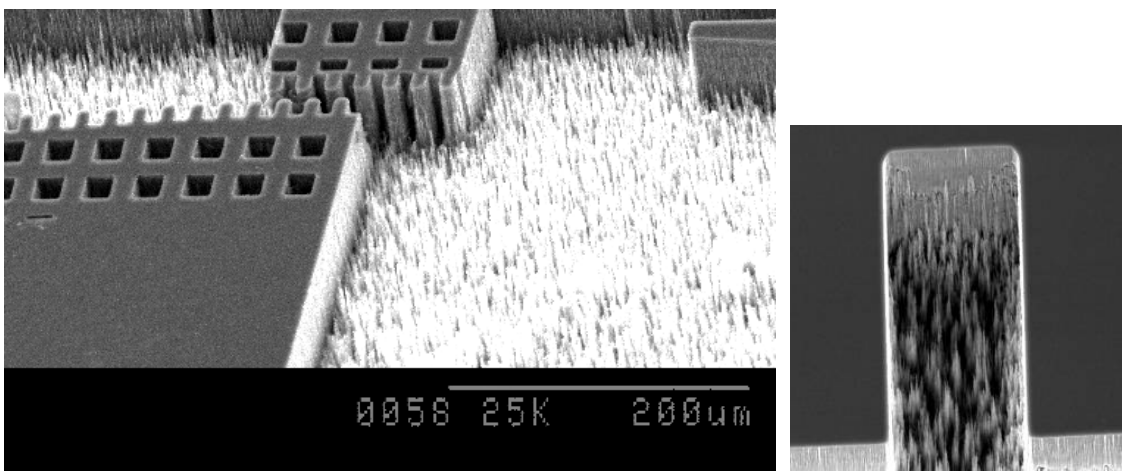

Figure 15. SEM images of black silicon at the bottom of a trench forming grass-like structures.

5.2.2.2 STS DRIE Malfunction

There were some glitches during the fabrication process. Notably, the STS DRIE Tool was damaged in a power outage. This required replacement of the turbo vacuum pump, as well as computer control malfunctions, which were repaired. Several qualification runs were performed to verify tool operation met specifications. Figure 16 shows the etch cross section profile. The red dotted line represents the desired etch profile. Figure 17 shows the smaller features were under-etched through the silicon device layer. Figure 18 shows a successful etch after adjusting the DRIE RF and cycling steps.

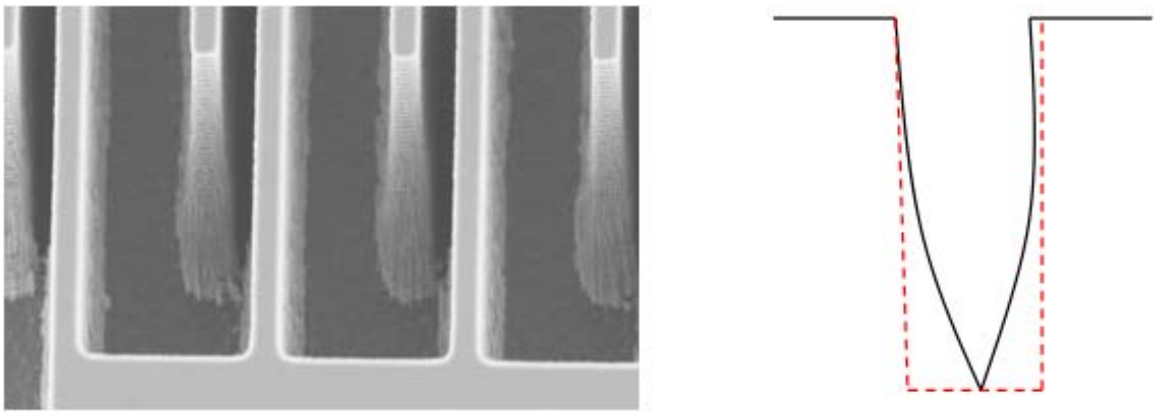

Figure 16. Left: Smaller features under-etched through the silicon device layer. Adjustments to the process parameters were needed to bring the process back to specification. Right: Etch cross section profile. The red dotted line represents the desired etch profile.

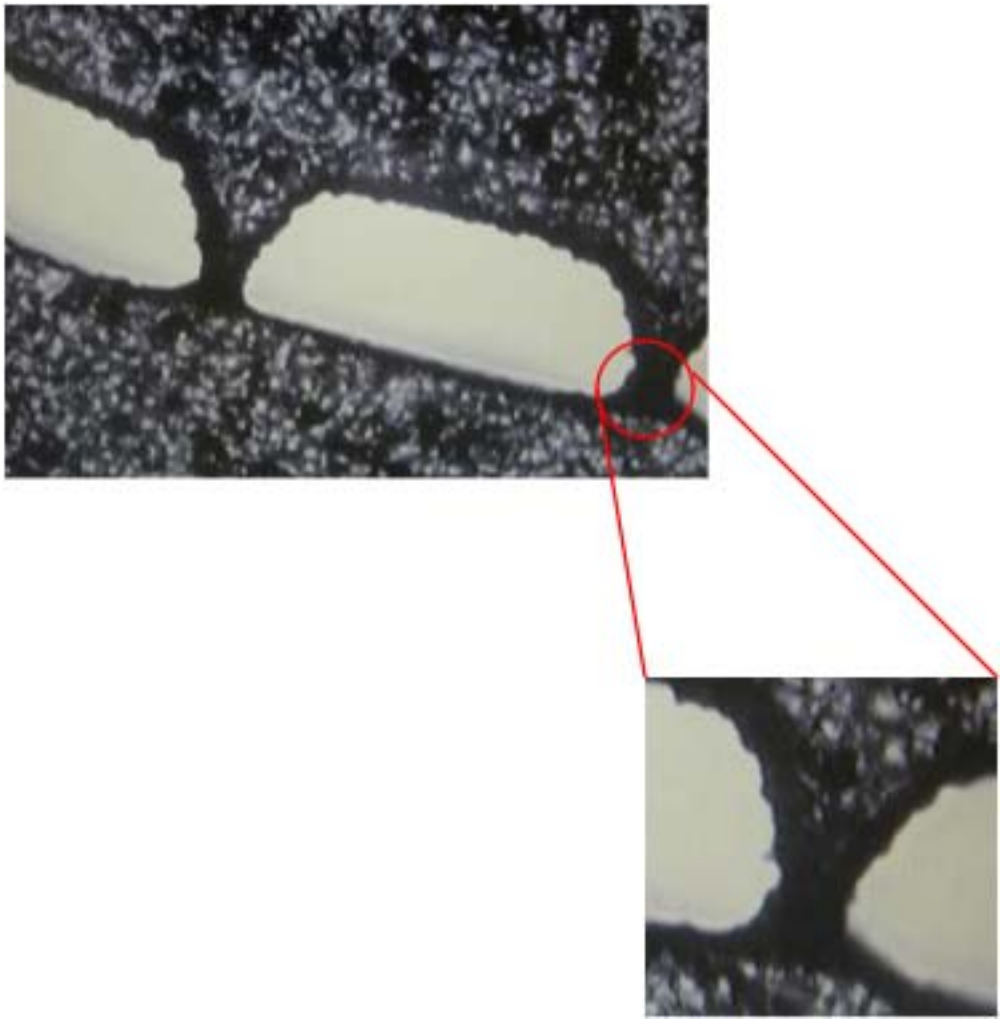

Figure 17. Micrograph showing the smaller features were not being etched all the way through the silicon device layer.

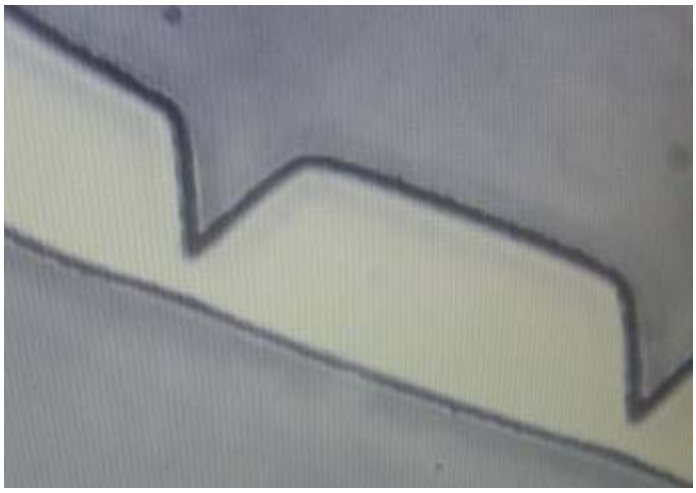

Figure 18. After adjusting the RF and cycle steps, silicon layers were successfully etched.

5.2.3 Integration and Testing

Once the circuit boards for the control electronics were fabricated and assembled, they were tested and then calibrated to operate with the MEMS gyroscope. Tuning involved setting the drive amplitude at a high enough level to get adequate response from the gyro, then the control electronics continuously monitor the resonant frequencies matching of the drive and sense modes and keep the quadrature error nulled out. Figure 19 shows the final circuit board, which contains the gyroscope mechanical sensing element and front-end low-noise amplification stages. The module is 0.75" diameter and requires only 5 volts power with a power consumption of 25mW. Figure 20 shows some initial gyroscope response measurements with the sensor being rotated back and forth.

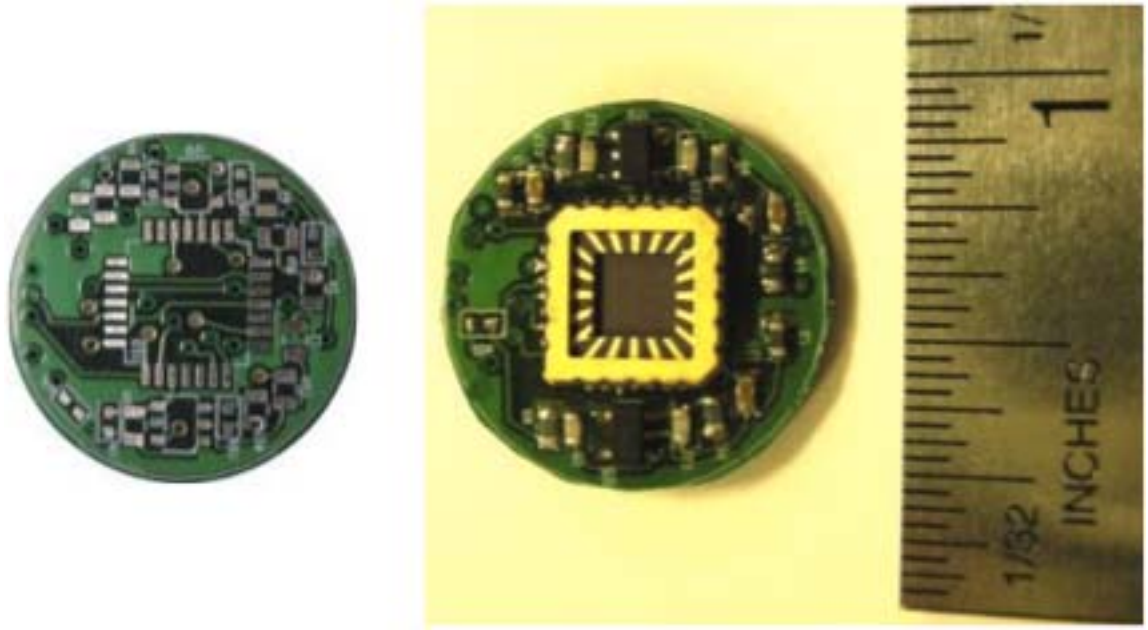

Figure 19. Designed printed circuit board, which contains the gyroscope mechanical sensing element and front-end low-noise amplification stages. The module is 0.75" diameter and requires just 5 volts power with a power consumption of 25mW.

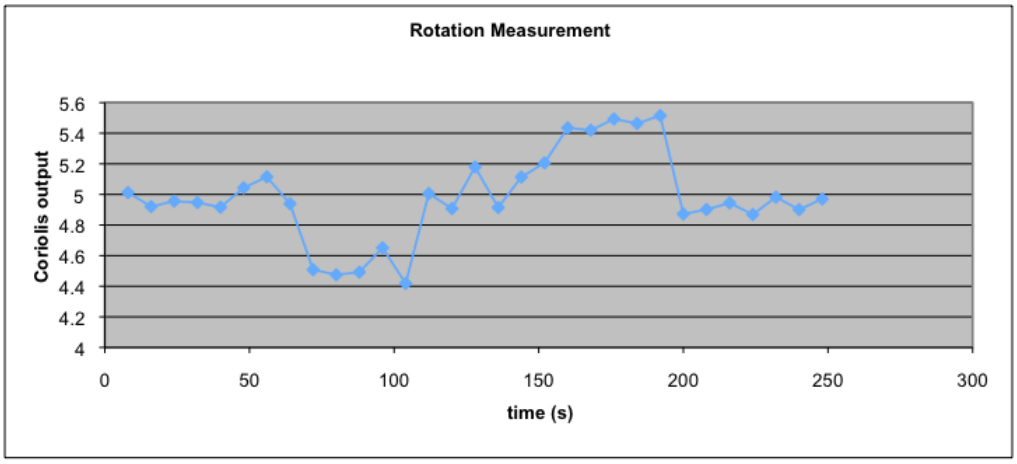

Figure 20. Rotation rate measurement

5.2.4 Noise Filtering / Cancellation

The control electronics can be characterized by using a frequency response analyzer that measures the signal levels along the frequency spectrum. The signal to noise ratio and the noise floor can be determined from these measurements. A noise floor of –86 dBV/rt Hz was measured.

Improvements were made to the control electronics to isolate the digital signals from the analog signals. This involved having separate power supplies for the digital electronics and the analog electronics. Also noise filtering was added at key points to suppress unwanted signals. The wiring and circuit boards were shielded to suppress picking up unwanted signals from nearby equipment. Improved results from the work reduced noise floor lowered to –99 dBV/rt Hz.

To effectively cancel the 1/f noise of the system, the team came up with a carouseling method integrated into the sensor module. The gyroscope is flipped orthogonally to the rotation sensing axis at a rate of about every 10 seconds. As shown in Figure 21, the rotation motor pulls a cable attached to the rotation module to rotate it back and forth 180 degrees.

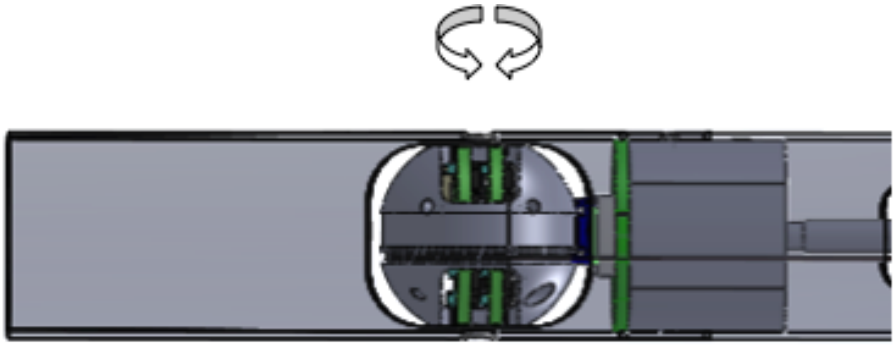

Figure 21. Design of the chip carouseling to cancel the 1/f noise.

5.2.5 Impact to Producers

It is imperative to bring reliable, domestic hydrocarbon reserves on-stream to help the United States reduce dependency on foreign oil. Domestic land formations are a critical national asset that needs to be developed to its maximum capacity. For example, at present, only a small percentage of Bakken reserves are anticipated to be recovered due in part to limitations with existing oilfield technology, including limitations in the accuracy of existing directional drilling technologies. The current Measurement While Drilling (MWD) technology, magnetometers, cannot be significantly improved since the errors are introduced by external sources.

The ability to install the sensor next to the drill bit substantially shortens response time, thereby improving accuracy and reliability. Because the system's errors do not accumulate, the range of the system can be substantially increased. Improved accuracy and reduced drilling time will accelerate the rate of commercial production, as well as exploration in emerging plays.

Gyroscopes are inertial sensors that measure rate of rotation (in °/sec or °/hr) without reference to external coordinates. MEMS vibratory gyroscopes are based on Coriolis acceleration, which arises in a rotating frame of reference and is proportional to the rate of rotation. The gyroscope is forced to vibrate (typically using inter-digitated comb drives) in the sense axis at its characteristic resonant frequency. When subjected to angular rotation, the vibrating mass senses Coriolis acceleration in the direction orthogonal to the drive direction and axis of rotation. This motion in the sense direction is directly proportional to the rate of rotation and is typically measured using capacitive sensing.

A MEMS gyro can significantly reduce drilling time for casing window cutting applications, intermediate radius re-entry applications and steering applications.

For the Casing Window Cutting application, Baker Hughes has estimated that adding a gyroscopes to the current MWD tool can save approximately $35,000 per well based on avoidance of the cost to plug back and re-drill (Table 1)[i]

For the Intermediate Radius Re-entry application, Baker Hughes has estimated that $115,000 per well can be saved based on net rig time savings and avoiding the need to plug back and re-drill the sidetrack (Table 2).

For steering applications, a direct cost savings cannot be estimated from eliminating the need to plug back and re-drill. However, improved accuracy will lead to a reduction in drilling time. In particular, directional measurement errors will accumulate from magnetometers whereas gyroscopes do not.

Table 1 — Wireline Gyro Replacement Example		
Casing Window Cutting	**Wireline**	**MWD Gyro**
Drilling Rig Daily Rental Rate	$60,000	$60,000
Directional Drilling Daily Rental Rate	$10,000	$10,000
Gyro Orienting (during 2 days)	13 hours	1 hour
Cost to Cut Window (during 2 days)	$140,000	$105,000
Rig Time Saved		12 hours
Window Cutting Savings		$35,000
Total Savings/well		**$35,000**

Table 2 — Wireline Gyro Replacement Example			
Intermediate Radius Re-Entry Kickoff	**MWD Alone**	**Steering Gyro ***	**MWD Gyro**
Drilling Rig Daily Rate	$60,000	$60,000	$60,000
Directional Drilling Daily Rental Rate	$10,000	$10,000	$10,000
Window Cost	$75,000	$75,000	$75,000
Drilling Time	1 day	1-1/2 days	1 day
Plug-Back Cost	$80,000		
Cost to Build Curve	$225,000	$180,000	$145,000
Window Cutting Savings (from Table 1)			-$35,000
Cost to Cut Window & Kickoff the Curve	$365,000	$320,000	$250,000
Total Savings/Well		**$45,000**	**$115,000**

* Assuming a wireline gyro steering tool is available

Table 2. Gyro replacement cost savings tables

5.2.6 Technology Transfer Efforts

Laserlith has designated 2.5% of the amount of the award for both the project and program level funding technology transfer activities. Throughout the project, Laserlith worked with RPSEA to develop and implement an effective Technology Transfer Program.

Technology transfer was achieved through the following efforts:

1. Project presentations and reports. Laserlith provided project presentations to update at the TAC meetings and participated in person or via web meeting. Laserlith provided monthly reports to RPSEA on a monthly basis.
2. Meetings:

   RPSEA TAC Meetings

   Bourgoyne Enterprises

   Potential commercialization partners and end users

Technology Transfer Focus

1. **Directional Drilling Service and Technology Providers**

   Laserlith worked closely with Ideal Aerosmith, who led the module development testing. Ideal Aerosmith has flourished long-term customer relationships with oil field service companies.

2. **End Users.**

   Oil company end users of the MEMS gyro technology can provide valuable insight on device functional requirements. In addition, oil company end users might offer future project support if that support facilitates keeping the MEMS gyro technology available through multiple service companies. Mainly through contacts with subject matter experts in the SPE Technical Section for Wellbore Positioning, the project attempted to develop relationships with potential end users.

3. **Technology Qualification**

   Initial qualification was the evaluation of microbump integration capability under high temperature and shock environment was performed by team member Ideal Aerosmith. While conducting the project and afterwards, the project team has seeked commercialization partners who can test the MEMS gyro module as an integrated component in a commercial MWD tool.

   The project leveraged the manufacturing infrastructure that had been assembled by team members, including:

1. Existing MEMS production line. The MEMS production line has the complete tool-set for the development and manufacturing of the MEMS gyroscope.
2. Manufacturing and test infrastructure for module production and testing at Ideal Aerosmith in East Grand Forks, Minnesota
3. Ongoing work by the team is to transfer the product design to a low-cost wafer-scale vacuum packaging process. Ramp-up of production facility will provide capacity of more than 1 million units per year.

The Laserlith team intends to develop, produce, market, sell, and support MEMS-based inertial guidance systems for directional drilling. The team includes the necessary development, manufacturing and support capabilities in-house, and is coordinating system development with oil drilling equipment companies.

5.3 Conclusions and Recommendations

Testing and improvements to the MEMS gyroscope will continue with a focus on further development of the control electronics and verify operation at high

temperatures. These results are necessary steps for building a complete sensor and test in a simulated down-hole environment.

Gyroscope System Improvements

Based on the test results, design revisions are being made to the gyroscope system to further improve performance. The MEMS gyroscope is being improved to make the design more tolerant to manufacturing variations. Additional optimizations have been made to the quadrature combs, proof mass suspension beams, and resonance modes.

Improvements are also being made to the gyro sense electronics to further reduce electrical noise. The gyro drive circuit is also being improved by making it more sensitive and responsive. A drive amplitude limiter will be added to prevent the proof mass from crashing, which has been one of the early failure mechanisms during testing.

Further recommendations include:

1. Reduce the size of the control electronics and continue to improve noise filtering
2. Begin design of the complete sensor for down-hole testing

6. BIBLIOGRAPHY

1. ElGizawy, Mahmoud et al, 2010, Continuous Wellbore Surveying While Drilling Utilizing MEMS Gyroscopes Based on Kalman Filtering, SPE 135602, SPE Annual technical conference and Exhibition, Sept. 19-22, Florence, Italy, pp: 1-2
2. Estes, R.A. and D.M. Epplin, 2000, Development of a robust gyroscopic orientation tool for MWD operations, SPE 63274, Proceeding of the Society of Petroleum Engineers Annual Technical Conference and Exhibition, Oct. 1-4, Dallas, TX, USA., pp: 1-13.
3. Noureldin. A. Et al, 2000, A New Borehole Surveying Technique for Horizontal Drilling Processes using One Fiber Optic Gyroscope and Three Accelerometers, IADC/SPE 59198, IADC/SPE Drilling Conference, Feb 23-25, New Orleans, LA, pp: 1-2
4. Thorogood, J. L., (1990), “Instrument performance models and their application to directional surveying operations,” Society of Petroleum Engineers, Drilling Engineering, V5(4), pp: 294-298

7. LIST OF ACRONYMS AND ABBREVIATIONS

AGC: automatic gain control

ASIC: application-specific integrated circuit

CTE: coefficients of thermal expansion

DRIE- Dry Reactive Ion Etching

LPCVD: low pressure chemical vapor deposition

MEMS: micro-electro-mechanical systems

SOI CMOS: silicon on insulator complementary metal-oxide semiconductor

TRL: technology readiness level

UAV: unmanned aerial vehicle

8. APPENDICES

None

9. References

[i] Estes, R. A. and Epplin, D. M. *Development of a Robust Gyroscopic Orientation Tool for MWD Operations*. SPE 63274, 2000.